Quantifying the Effects of the Influence of a Tungsten Long-rod Projectile into Confined Ceramics at High-velocity Impact

Tara J. Gorsich and Douglas W. Templeton

US Army RDECOM-TARDEC, 6501 E. Eleven Mile Road, MS 263, Warren, MI 48397-5000, USA, Tara.Gorsich@us.army.mil and Douglas.Templeton@us.army.mil

High performance modeling of brittle materials is an efficient, inexpensive, time-saving solution for optimal design of armor systems. Quantifying the effects of high-velocity projectiles into brittle materials provides an armor resolution for the critical need of ballistic protection against lethal threats. The analysis modeled a cylindrical, tungsten carbide blunt projectile into four confined, ceramic materials at a high velocity impact. The finite element simulations were performed using Elastic Plastic Impact Code (EPIC) [Johnson (2006)], which simulates the failure and particle breakup of the target once the long-rod penetrator strikes at high-velocity impact. The history of the nose penetration of the projectile will be computed to establish the most advantageous design condition for future vehicle development. Damage computations will also be conducted to demonstrate how the confined, brittle samples behave. The study shows that silicon carbide and boron carbide are the optimal candidates to consider when selecting the best armor performance from the four configurations. A numerical comparison was made between a pyroceram confined and unconfined configuration and ascertains approximately a twelve percent increase in ballistic performance of the confined sample. The computations will offer the researcher data to accurately formulate armor to protect the survivability of the ground vehicle, and most importantly, the soldier.

INTRODUCTION

Development of lightweight, high performance armor for ballistic protection is a critical need for soldier and ground platform protection. Experimental range testing of projectiles and ballistic armor can be expensive, time-consuming, and an environmental hazard; however, it is necessary to verify the actual behavior of such systems. Modeling and simulation (M&S) allows the researcher to analyze design conditions in a highly interactive and visual environment and gives details about the impact process which

Report Documentation Page		*Form Approved* *OMB No. 0704-0188*

Public reporting burden for the collection of information is estimated to average 1 hour per response, including the time for reviewing instructions, searching existing data sources, gathering and maintaining the data needed, and completing and reviewing the collection of information. Send comments regarding this burden estimate or any other aspect of this collection of information, including suggestions for reducing this burden, to Washington Headquarters Services, Directorate for Information Operations and Reports, 1215 Jefferson Davis Highway, Suite 1204, Arlington VA 22202-4302. Respondents should be aware that notwithstanding any other provision of law, no person shall be subject to a penalty for failing to comply with a collection of information if it does not display a currently valid OMB control number.

1. REPORT DATE **29 JAN 2008**	2. REPORT TYPE **N/A**	3. DATES COVERED **-**

4. TITLE AND SUBTITLE **Quantifying the Effects of the Influence of a Tungsten Long-rod Projectile into Confined Ceramics at High-velocity Impact**	5a. CONTRACT NUMBER
	5b. GRANT NUMBER
	5c. PROGRAM ELEMENT NUMBER
6. AUTHOR(S) **Gorsich,Tara,J; Templeton,Douglas,W**	5d. PROJECT NUMBER
	5e. TASK NUMBER
	5f. WORK UNIT NUMBER

7. PERFORMING ORGANIZATION NAME(S) AND ADDRESS(ES) **US Army RDECOM-TARDEC 6501 E 11 Mile Rd Warren, MI 48397-5000**	8. PERFORMING ORGANIZATION REPORT NUMBER **18527**

9. SPONSORING/MONITORING AGENCY NAME(S) AND ADDRESS(ES)	10. SPONSOR/MONITOR'S ACRONYM(S) **TACOM/TARDEC**
	11. SPONSOR/MONITOR'S REPORT NUMBER(S) **18527**

12. DISTRIBUTION/AVAILABILITY STATEMENT
Approved for public release, distribution unlimited

13. SUPPLEMENTARY NOTES
Presented at the 32nd International Conference & Exposition on Advanced Ceramics and Composites - 27 JAN to 1 FEB 2008, Daytona Beach, FL, The original document contains color images.

14. ABSTRACT

15. SUBJECT TERMS

16. SECURITY CLASSIFICATION OF:			17. LIMITATION OF ABSTRACT **SAR**	18. NUMBER OF PAGES **8**	19a. NAME OF RESPONSIBLE PERSON
a. REPORT **unclassified**	b. ABSTRACT **unclassified**	c. THIS PAGE **unclassified**			

Standard Form 298 (Rev. 8-98)
Prescribed by ANSI Std Z39-18

would be difficult to experimentally obtain. M&S also offers specifics into the penetration process and damage accumulation and provides information for the development of an optimized, experimental test plan, reducing both cost and schedule. This computational study quantifies the ballistic efficiency for four, confined brittle materials and gives an understanding about the physical process taking place. This analysis will also compare an unconfined and confined sample and evaluate and compare the response.

Attractive materials for use in armor systems are ceramics due to their superior hardness and compressive strength. It is important to confine the ceramic fragments and to absorb the kinetic energy of the projectile and the ceramic debris during target penetration and increase the ballistic efficiency. Confinement is also useful for multiple shot testing and recovery work. Ceramics have a low density, which in turn reduces the weight, high bulk and shear moduli that prevent large deformations, and a high yield stress to preserve resistance to failure. Unfortunately, ceramics are brittle materials that produce extensive fragmentation caused by tensile waves generated by the compressive waves reflected from the free surfaces. Carrying out a variety of parametric studies, in which only one parameter can be altered, clearly demonstrates each design limitation and the overall effects of the process of penetration mechanics and damage.

MODELING APPROACH

The Lagrangian hydrocode, EPIC, was use to perform the computations in this parametric study. Lagrangian methods, in which the finite difference grid is fixed with the material, are more frequently utilized for this particular type of structural evaluation. Free and contact surfaces between various materials remain distinct throughout the calculation and the mesh deforms with the evolutionary flow. The four cylindrical, confined ceramic specimens investigated were aluminum nitride, boron carbide, 9606 pyroceram, and silicon carbide. The confining sleeve was modeled with RHA and had a diameter and length of 5 and 50 mm, respectively. The front and rear plug materials were both RHA with a diameter and length of 25 and 10 mm. The RHA sleeve was welded to correlate with experimental approaches. The tungsten impactor of interest was modeled as a blunt, long rod with a diameter of 2 mm and length of 80 mm. Figure 1 illustrates the modeled geometry of the projectile used in the analysis. An initial computation involving a SiC sample with a specific geometric configuration was performed based on the work by Holmquist to compare computed penetration results with experimental findings (Holmquist [2002]) and gain insight into the penetration process using confined samples.

The problem was assumed to be 2-D axisymmetric, using the Johnson-Holmquist I (Johnson [1992]), Johnson-Holmquist II (Johnson [1994]), and Johnson-Holmquist-Beissel (Johnson [2003]) constitutive models. The JH-1 model did not allow for continuing damage; whereas, the JH-2 constitutive equation includes the effect of damage and residual material strength (as a function of the representative variables) and the resulting bulking during the compressive failure of a ceramic material. The JHB equation is more recently developed and better describes the hydrostatic pressure including a phase

change from additional experimental data for various ceramics. In this analysis, the JH-1 model was used for the carbide and pyroceram, the JH-2 model was employed for the boron carbide, and the JHB model was applied for the aluminum nitride and silicone carbide. Tables I, II, and III below show the material model constants used for the JH-1, JH-2, and JHB ceramic cases.

PROJECTILE CLASSIFICATION:

-- Material: Tungsten
-- Length: 80 mm
-- Diameter: 2 mm
-- **Velocity: 1645 m/sec**

CONFINED TARGET CLASSIFICATION:

-- Plug material: RHA
-- Plug length: 10 mm
-- Plug diameter: 25 mm

-- Sleeve material: RHA
-- Sleeve length: 70 mm
-- Sleeve diameter: 5 mm

-- Sample materials: AlN, B_4C, pyroceram, and SiC
-- Sample length: 50 mm
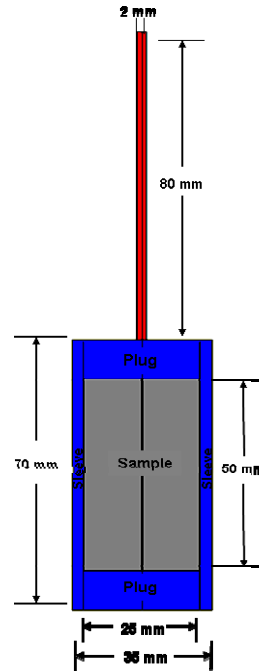-- Sample diameter: 25 mm

Figure 1: Original configuration (t = 0 μs) of the confined samples

Table I. Material constants using the JH-1 constitutive model	
	Pyroceram
Density (Kg/m^3)	2608
Specific Heat (J/kg-^{o}C)	975
Shear Modulus (GPa)	47
Intact Strength 1 (GPa)	3.27
Intact Pressure 1(GPa)	1.20
Intact Strength 2 (GPa)	4.79
Intact Pressure 2 (GPa)	4.12
Strain Rate Coefficient, C	0.01
Tensile Strength (GPa)	0.24
Maximum Failed Strength (GPa)	3.11
Bulk Modulus, K1 (GPa)	76.0
Pressure Constant, K2 (GPa)	76.00
Pressure Constant, K3 (GPa)	0.000
Damage Constant, D1	4.1
Damage Constant, EFMAX	0.005

Table II. Material constants using the JH-2 constitutive model	
	B$_4$C
Density (Kg/m^3)	2510
Specific Heat (J/kg-^{o}C)	999
Shear Modulus (GPa)	196
Strength Coefficient, A	0.93
Strength Coefficient, N	0.67
Strength Coefficient, B	0.70
Strength Coefficient, M	0.85
Strain Rate Coefficient, C	0.005
Tensile Strength (GPa)	0.26
Normalized Fracture Strength (GPa)	0.20
HEL (GPa)	19.0
HEL Pressure (GPa)	8.71
HEL Volumetric Strain (GPa)	0.041
HEL Strength (GPa)	15.4
Damage Constant, D1	0.001
Damage Constant, D2	0.50
Bulk Modulus, K1 (GPa)	233
Pressure Constant, K2 (GPa)	-593
Pressure Constant, K3 (GPa)	2800

Table III. Material constants using the JHB constitutive model		
	AlN	**SiC**
Density (Kg/m^3)	3226	3215
Specific Heat (J/kg-^{o}C)	735	839
Shear Modulus (GPa)	127	193
Intact Strength (GPa)	4.31	4.92
Pressure (GPa)	1.50	1.50
Maximum Strength (GPa)	5.50	12.2
Strain Rate Coefficient, C	0.013	0.009
Failed Strength (GPa)	0.09	0.09
Tensile Strength, T (GPa)	0.45	0.75
Maximum Failed Strength (GPa)	0.20	0.20
Bulk Modulus, K1 (GPa)	201	220
Pressure Constant, K2 (GPa)	260	361
Pressure Constant, K3 (GPa)	0	0
Damage Constant, D1	0.16	0.16
Damage Exponent, N	1.00	1.00

COMPUTED RESULTS

EPIC was accessed and the analysis was carried out on TARDEC's high performance computing (HPC) system on a 32-processor SGI® Onyx® 350 for the batch-oriented computations. The HPC's hardware was used to provide the computational power necessary to perform this analysis and save time. Figure 2 displays the final geometry associated with the impact at 100 μs into the four, brittle targets. EPIC is able to automatically convert the 2D axisymmetric finite elements into meshless particles as they become severely distorted, which can be easily identified in the figure. Majority of the grid remains as finite elements, and this allows for an accurate and efficient solution for the less distorted portion of the problem (Johnson [2001]).
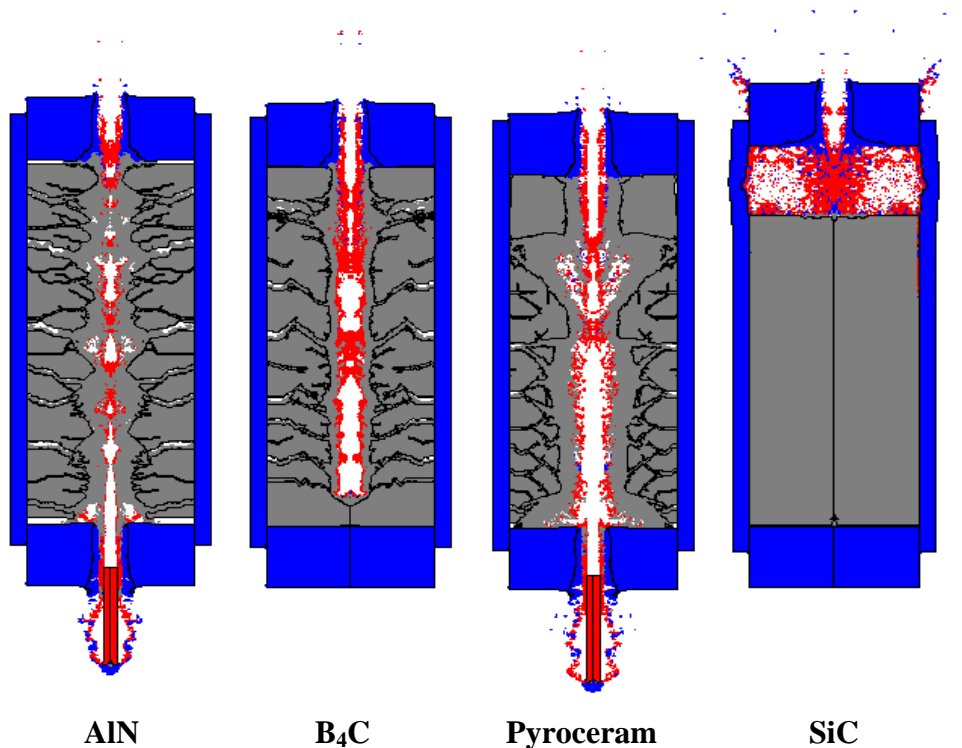

| AlN | B$_4$C | Pyroceram | SiC |

Figure 2: Final geometry associated the impact velocity of 1645 m/sec into the four confined specimens

At 10 μs, the penetrator completely shears through the RHA front plug and reaches the face of the ceramic samples. All the ceramics begin to absorb the kinetic energy and fracture and lateral cracking of the ceramic becomes visible, apart from the SiC sample. A cavity forms in the targets, the long rod starts to erode away, and the spall plane becomes visible at the front surface. The ceramics are relatively incompressible and there was no free volume for the comminuted material to expand into except the penetration hole itself. The rod sheared through RHA top and back plate by 90 μs and

completely exits the specimen within the confined perimeter for all the cases, with the exception of the boron carbide and silicon carbide. The rod completely eroded within and is arrested by the B_4C target configuration. Interface defeat occurs in the SiC sample, or the condition in which the projectile completely dwells on the surface, but does not penetrate.

Fig. 3 displays the damage results of the normal impact of the projectile at 50 µs into the confined ceramic targets with a 50 mm. thick ceramic sample at 1645 m/sec.
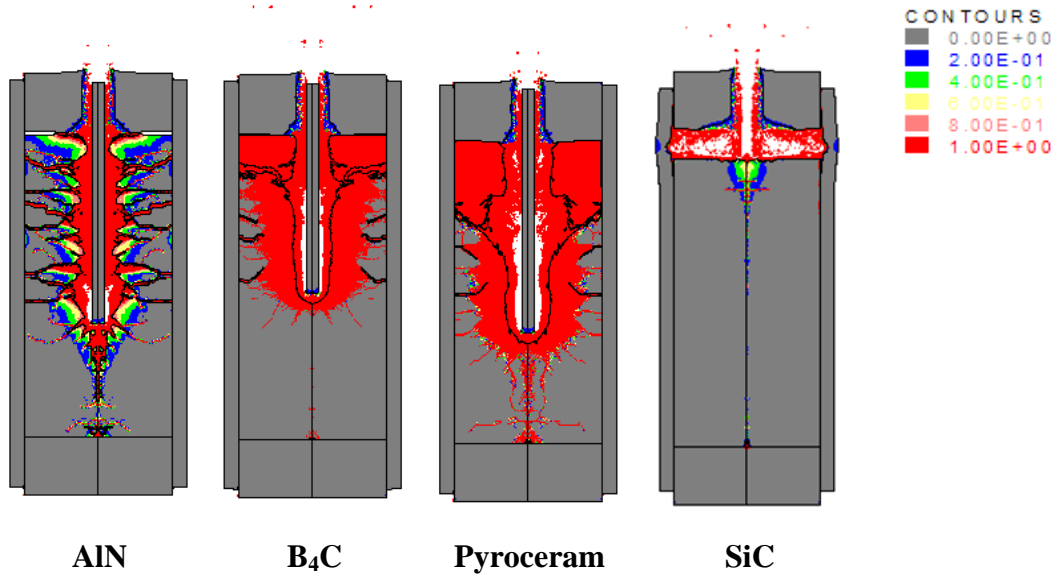

Figure 3: Damage accumulated from the impact velocity of 1645 m/sec into the four confined samples

The magnitude of the compressive stress wave exceeds the local dynamic strength of the material, and damage begins to accumulate through the formation of cracks under the impact location. By 10 µs, a comminuted zone is formed ahead of the tungsten projectile rod due to the intense stress conditions. The fracture front travels through the material and a visible conoid of pulverized material begins to form under the impact location for the first four samples, with the exception of the SiC target. It is obvious the silicon carbide sample has the best ballistic efficiency. A second or third choice material for armor solutions would be boron carbide or aluminium nitride, respectively.

A time history ASCII file was updated to obtain the data corresponding to the z-coordinate of the penetrator in order to trace the nose into the target. Figure 4 shows the time history of the data acquired from the computations performed.
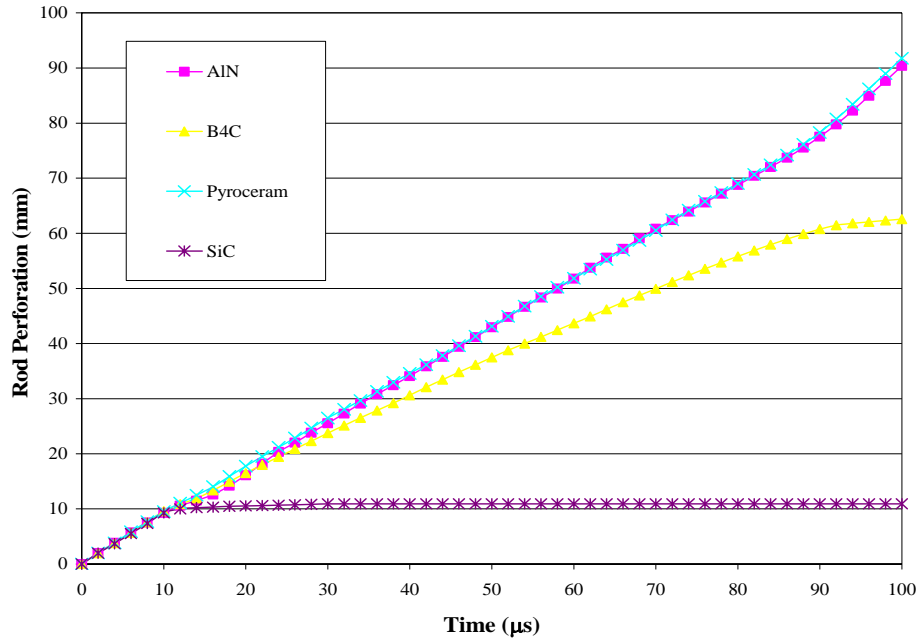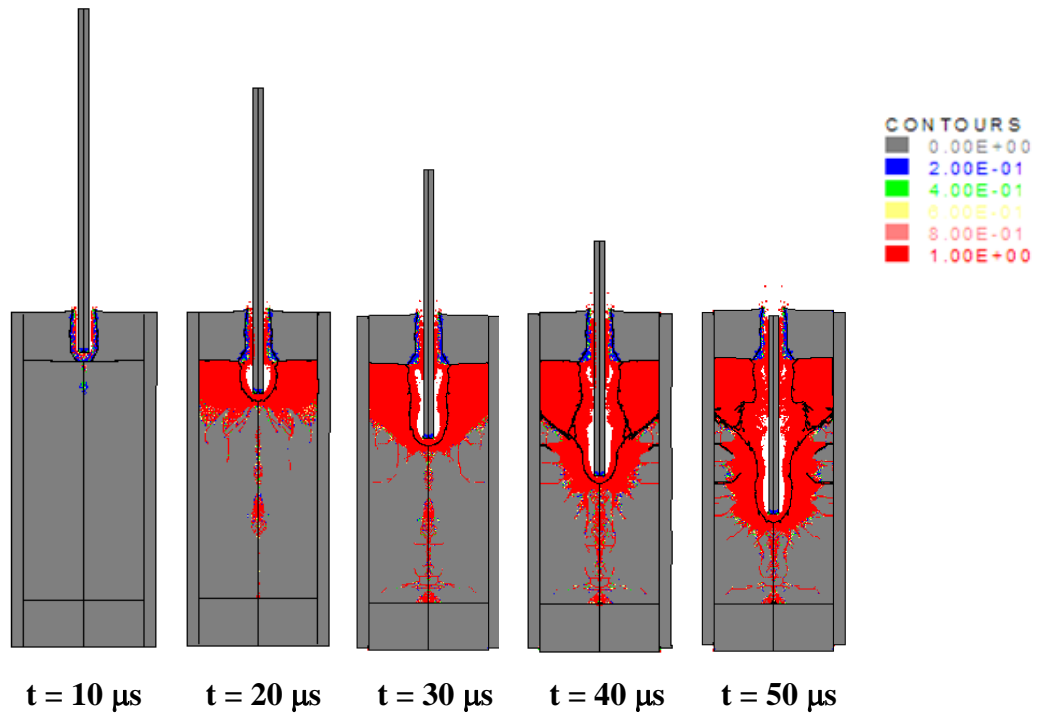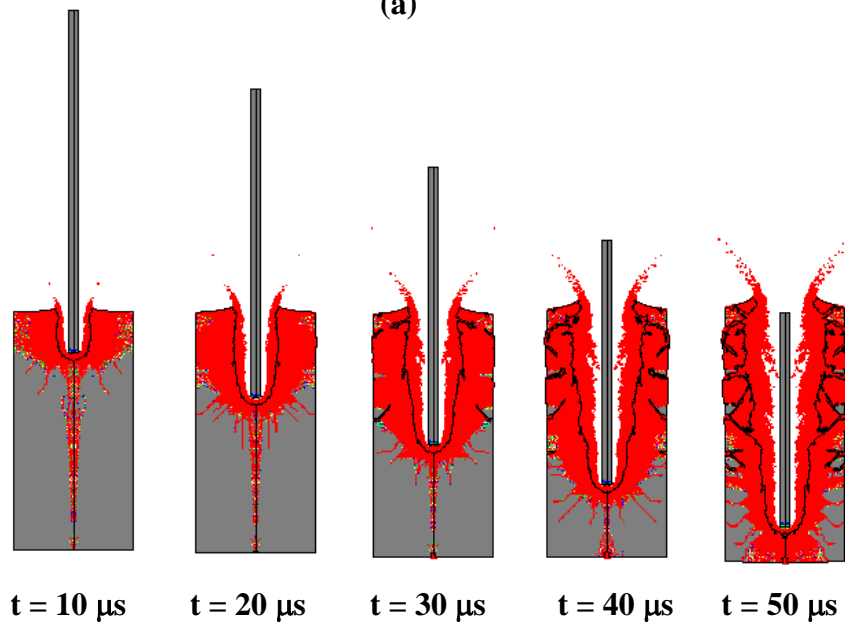
Figure 4: Time history plot of the nose coordinates for the long rod into the targets for the four confined configurations

It is important to achieve optimum ballistic performance of ceramic targets to aid in the evaluation of the response. The pyroceram configuration was chosen to compare confinement and unconfined targets, because the tungsten penetrator remains mostly rigid during the computation. Table IV shows the tungsten rod's nose coordinates into the actual ceramics. Figures 5 (a) and (b) below demonstrate the penetration effects and damage accumulation of a confined and unconfined specimen from 10 to 50 μs, respectively. It is obvious that confining the ceramic significantly increases the ballistic efficiency. By 60 μs, the rod completely exits the rear of the unconfined sample; whereas, the 1645 m/s threat is completely arrested in the confined ceramic. It is obvious that confining configurations improve the mechanical properties by inhibiting the failure mechanisms. The restraints limit the flow of pulverized ceramic debris and can be used to increase the resistance to penetration. There is approximately a 12% increase in ballistic efficiency for the confined sample.

Table IV: Nose coordinates of tungsten rod into actual ceramics		
Time (μs)	Confined sample (mm)	Unconfined sample (mm)
0	0	0
10	7.772	9.552
20	16.489	18.389
30	24.593	27.518
40	33.139	36.579
50	41.854	45.794

CONTOURS
⬛	0.00E+00
🟦	2.00E-01
🟩	4.00E-01
🟨	6.00E-01
🟧	8.00E-01
🟥	1.00E+00

t = 10 μs   t = 20 μs   t = 30 μs   t = 40 μs   t = 50 μs

(a)

t = 10 μs   t = 20 μs   t = 30 μs   t = 40 μs   t = 50 μs

(b)

Figure 5: Damage progression in (a) confined and (b) unconfined pyroceram computation at 1645 m/s

SUMMARY AND CONCLUSION

Computations of a tungsten long-rod penetrator impacting four confined ceramics at high-velocity impact were conducted to propose a baseline to compare ballistic performance. Modeling and simulation of ballistic events offers an advanced understanding of the failure mechanisms and is important for developing improved models and for designing better armor systems. Numerical simulation also makes the requirement to produce hardware for experimental testing and validation more efficient. In this study, EPIC was employed to capture the final geometry and damage associated with the four confined, brittle samples. Confined silicon carbide, boron carbide, or aluminum nitride are the optimal candidates to consider when selecting the best armor performance. The response of a confined and unconfined pyroceram sample was compared, and the results show there is a significant increase in the ballistic performance of the confined ceramic. Additional study of such confined configurations is needed and could provide valuable information in guiding the development of vehicle armor designs.

REFERENCES

Johnson, G.R. and Holmquist, T.J. A Computational Constitutive Model for Brittle Material Subjected to Large Strains, High Strain Rates, and High Pressures. *Shock-wave and High Strain-rate Phenomena in Materials*, 1992.

Johnson, G.R. and Holmquist, T.J. An Improved Computational Constitutive Model for Brittle Materials. *High-Pressure Science and Technology*, 1993. American Institute of Physics Press, 1994.

Johnson, G.R., Stryk, R.A, Beissel, S.R., and Holmquist, T.J. Conversion of Finite Elements into Meshless Particles for Penetration Computations Involving Ceramic Targets. *Shock Compression of Condensed Matter*, 2001.

Holmquist, T.J. and Johnson, G.R. Response of Silicon Carbide to High Velocity Impact. *Journal of Applied Physics*, 91, 2002.

Johnson, G.R., Holmquist, T.J., and Beissel, S.R. Response of Aluminum Nitride (Including a Phase Change) to Large Strains, High Strain Rates and High Pressure. *Journal of Applied Physics*, 99, 2003.

Johnson, G.R., Beissel, S.R., Gerlach, C.A., Stryk, R.A., Holmquist, T.J., Johnson, A.A., Ray, S.E., and Arata, J.J. *User Instructions for the 2006 Version of the EPIC Code*, Network Computing Services, Inc., Minneapolis, Minnesota, 2006.